Implementing Hybrid Electromagnetic Models in Time-Domain Simulations

A. C. S. Lima, R. A. R. Moura, P. H. N. Vieira, M. T. Correia de Barros, and M. A. O. Schroeder

***Abstract*—This work proposes time-domain modeling for non-uniform conductors such as those found in very short lines, i.e, when the length of the actual circuit is in the same order of magnitude as the height of the conductors, or when the conductors are arbitrarily oriented. They are represented via the so-called Hybrid Electromagnetic Model (HEM) allowing an implementation in time-domain simulation programs such as EMTP. The procedure is based on obtaining an equivalent nodal admittance matrix for the system using HEM and then apply a frequency domain fitting assuming a rational approximation. Using a passivity enforcement routine, this model can be interfaced with any EMT type of programs. Two test cases are considered to evaluate the time responses. One uses a comparison with already published experimental results, and the other uses a comparison with simulations carried out in the frequency domain using the Numerical Laplace Transform (NLT) .**

***Keywords*—Grounding System, Lightning Protection, Rational Approximation.**

I. Introduction

THERE is an increasing need to evaluate higher frequency phenomena in electromagnetic transient analysis. Typically, this is the case of lightning related analysis, electromagnetic compatibility and more recently transients involving power electronics based systems. In some of these scenarios, the assumptions related to a quasi-TEM propagation do no hold, and more complex modeling should be considered [1]. A full-wave model is then needed and one has to deal with an integral equation to be solved. If a conductor has a constant height and is close to a lossy interface it is possible to solve the actual integral equation [2]. Unfortunately this approach is not suitable to multi-phase configurations or when the length of the actual circuit is in the same order of magnitude as the height of the conductors. Alternatively, one may use approximate approaches to solve the integral equation as the Method of Moments (MoM) [3] or use predefined values for the unknown propagation constant in the integral equation [4].

This work was partially supported by INERGE (Instituto Nacional de Energia Elétrica), CNPq (Conselho Nacional de Desenvolvimento Científico e Tecnológico), CAPES (Coordenação de Aperfeiçoamento de Pessoal de Nível Superior),FAPEMIG (Fundação de Amparo à Pesquisa do Estado de Minas Gerais) and FAPERJ (Fundação Carlos Chagas Filho de Amparo à Pesquisa do Estado do Rio de Janeiro).

A. C. S. Lima, is with Universidade Federal do Rio de Janeiro, COPPE/UFRJ, P.O. Box. 68504, 21945-970, Rio de Janeiro, RJ Brazil, R. A. R. Moura, P. H. N. Viera, M. A. O. Schroeder are with Universidade Federal de São João del Rey, Minas Gerais, Brazil. M. T. Correia de Barros is with Universidade de Lisboa, Instituto Superior Técnico, Lisboa, Portugal, emails: acsl@dee.ufrj.br, pedrohnv@hotmail.com, moura@ufsj.edu.br, schroeder@ufsj.edu.br, teresa.correiadebarros@tecnico.ulisboa.pt.

Paper submitted to the International Conference on Power Systems Transients (IPST2019) in Perpignan, France June 17-20, 2019.

The inclusion of MoM-based models on EMTP-type simulations represents a challenge and the frequency domain seems to be the preferable choice, see for instance [5]. Previous attempts to include wideband grounding systems have focused on either using uniform [6] or nonuniform line modeling [7]. To the best of the authors knowledge, little has been done regarding the actual representation of the conductor sags.

In this work, a distinct approach is sought. First, we consider the so-called Hybrid Electromagnetic Model (HEM) [8] for obtaining the wideband impedances for thefrequency range of interest. After obtaining the equivalent nodal admittance matrix, a rational approximation is carried out using the so-called Vector Fitting algorithm [9]–[11] which can then be directly integrated in any EMTP-type of program via recursive convolution [12] or using an equivalent RLC circuit [13]. However, the latter is prone to inaccuracies due to the limited accuracy of RLC branches [14].

The paper is organized as follows. Section II describes the formulation of the impedance matrices based on MoM and their assembly in an equivalent nodal admittance matrix. Section III presents the test cases, frequency and time domains analyzes are carried out for the assessment of the proposed approach. The main conclusions of this work are shown in Section IV.

II. Mathematical Modeling

A. Impedance Matrices Formulation

Consider, initially, an arbitrary oriented lossless electrode with radius a and length L_i and another electrode with same radius but with length L_k immerse in a medium with conductivity σ, permeability μ and permittivity ε, as depicted in Fig. 1. A filamentary current $\mathbf{I}$ is injected at the center of conductor i. The electrical field at an arbitrary point at the surface of electrode k is then given by

$$\mathbf{E} = \frac{j\omega\mu\,\mathbf{I}}{4\pi}\int\limits_{L_i}\frac{\exp\left(-\gamma r\right)}{r}\cos\phi\,d\xi \tag{1}$$

where r is the distance between an arbitrary infinitesimal element at the center of electrode i to an arbitrary point at the surface of electrode k, ϕ is the angle between vectors associated with L_i and L_k, $\gamma = \sqrt{j\omega\mu\left(\sigma + j\omega\varepsilon\right)}$.

Integrating (1) along the electrode surface leads to the induced voltage $\mathbf{V}_L$ due to the filamentary current $\mathbf{I}$. The longitudinal impedance is then given by,

$$Z_{L_{ik}} = \frac{\mathbf{V}_L}{\mathbf{I}} = \frac{j\omega\mu}{4\pi}\int\limits_{L_i}\int\limits_{L_k}\frac{\exp\left(-\gamma r\right)}{r}\cos\phi\,d\xi d\zeta \quad . \tag{2}$$

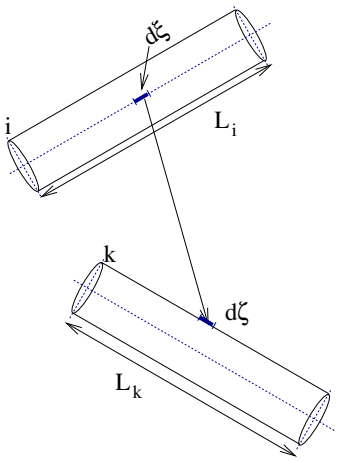

Fig. 1. Finite length lossless electrodes in a uniform medium.

In the case of the self-impedance, the distance is from the center of the electrode to an arbitrary point at its surface as depicted in Fig. 2, i.e.,

$$Z_{L_{ii}} = \frac{\mathbf{V}_L}{\mathbf{I}} = \frac{j\omega\mu}{4\pi} \int_{L_i}\int_{L_i} \frac{\exp(-\gamma r)}{r} d\xi d\zeta \quad . \tag{3}$$

The effect of the conductor losses can be considered by adding to Z_L the internal impedance Z_{in} calculated using the well-known expression

$$Z_{in} = \frac{j\omega\mu}{2\pi\gamma_c a} \frac{I_0(\gamma_c a)}{I_1(\gamma_c a)} \tag{4}$$

where $\gamma_c \approx \sqrt{j\omega\mu_c\sigma_c}$ is the propagation constant of the conductor as in most conductors $\sigma_c \gg \omega\varepsilon_c$ for all frequencies of interest, μ_c is the permeability of the electrode, σ_c is its conductivity, and ε_c is the permittivity of the electrode.

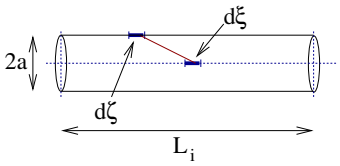

Fig. 2. Procedure to obtain the self-impedance for electrode i in a uniform medium.

The elements of the shunt (transversal) impedance matrix can be obtained from the electric scalar potential. First, we need to consider the density of the shunt current $\mathbf{I}_T$ injected into the external medium from conductor i, $\mathbf{J} = \frac{\mathbf{I}_T}{L_i}$. This current is also referred as leakage current. The electric scalar potential then can be written as

$$\varphi = \frac{1}{L_i} \frac{\mathbf{I}_T}{4\pi(\sigma + j\omega\varepsilon)} \int_{L_i}\int_{L_k} \frac{\exp(-\gamma r)}{r} d\xi d\zeta \tag{5}$$

integrating (5) and dividing it by L_k gives the average electric scalar potential in conductor k, $\mathbf{V}_T$ due to a transverse current from electrode i. Then the transversal impedance between electrodes i and k is given by

$$Z_{T_{ik}} = \frac{\mathbf{V}_T}{\mathbf{I}_T} = \frac{1}{L_i L_k} \frac{1}{4\pi(\sigma + j\omega\varepsilon)} \int_{L_i}\int_{L_k} \frac{\exp(-\gamma r)}{r} d\xi d\zeta \quad . \tag{6}$$

The self-elements of the shunt impedance matrix can be obtained directly as

$$Z_{T_{ii}} = \frac{1}{L_i L_i} \frac{1}{4\pi(\sigma + j\omega\varepsilon)} \int_{L_i}\int_{L_i} \frac{\exp(-\gamma r)}{r} d\xi d\zeta \quad . \tag{7}$$

where r is a distance from a point at the electrode center to its surface.

B. Effect of air-soil interface

A rigorous solution to represent the air-soil interface can be obtained if the actual spherical wave is considered through a series expansion of plane waves and then obtaining a coherent set of reflection and refraction coefficients for each one of these plane waves, see for instance [15, sec. 7.6]. Unfortunately, this approach is very time-consuming and simpler approaches can be considered. To do so, first one has to consider the medium where the voltages and currents are to calculated.

For instance, if we consider a grounding system, the electrodes are in a lossy medium and the approach is rather distinct from the one we should use if the electrodes are in air near a lossy interface. In the case of buried bare electrodes, if the distance from the electrodes is sufficiently larger than the electrode radius we can use simple charge/current images. Recently, it was shown in [16,17] that for several practical applications of grounding electrodes, charge images might suffice which implies that there will be an image for $\mathbf{Z}_T$, with $\mathbf{Z}_L$ remaining the same. The elements for the additional matrix are given by

$$\overline{Z}_{T_{j\overline{k}}} = \frac{\Gamma}{L_i \overline{L}_k} \frac{1}{4\pi(\sigma + j\omega\varepsilon)} \int_{L_i}\int_{\overline{L}_k} \frac{\exp(-\gamma r)}{r} d\xi d\zeta \quad . \tag{8}$$

where $\overline{L}_k$ is an image of electrode L_k and

$$\Gamma = \frac{\sigma_1 + j\omega\varepsilon_r\epsilon_0 - j\omega\epsilon_0}{\sigma_1 + j\omega\varepsilon_r\epsilon_0 + j\omega\epsilon_0} \quad . \tag{9}$$

The final transverse impedance is then given

$$\mathbf{Z}_{T_{new}} = \mathbf{Z}_T + \overline{\mathbf{Z}}_T \tag{10}$$

where the elements of $\mathbf{Z}_T$ are given by (6) and $\overline{\mathbf{Z}}_T$ are given by (8).

In the case of electrodes above a lossy medium. The scenario is slightly different. For $\mathbf{Z}_T$, one may resort to a series of complex images, see for details [18]. Fortunately, in a first approximation, it is possible to consider a single complex image at a distance d_i given by

$$d_i = \frac{2}{\sqrt{\gamma_s^2 - \gamma_0^2}} \tag{11}$$

where γ_s is the ground propagation constant and $\gamma_0 = j\omega/c$, being c the speed of light. If we consider $\gamma_s \gg \gamma_0$ in the

procedure to derive d_i, it becomes $di = 1/\gamma_s$ which is the same result as the one used in the complex ground plane [19]. For $\mathbf{Z}_L$, it is sufficient to consider the transmission coefficient between air and the lossy medium.

C. Assembly of Equivalent Nodal Admittance Matrix

After obtaining $\mathbf{Z}_T$ and $\mathbf{Z}_L$, we need to assemble them in order to derive an equivalent nodal admittance matrix. So consider that electrode i is represented by nodes "1" and "2", while "3" and "4" are the nodes associated with electrode k. First, it is assumed that with respect to the transverse (shunt) current $\mathbf{I}_T$ the voltage at the electrode can be given by the average of its transverse voltage, thus it is possible to write

$$\mathbf{Z}_T \cdot \mathbf{I}_T = \mathbf{m}_A \cdot \mathbf{V}_n \tag{12}$$

where $\mathbf{m}_A$ is a matrix defined as

- $\mathbf{m}_A(i,k) = 0.5$, if node i is connected to segment k,
- $\mathbf{m}_A(i,k) = 0$, otherwise.

Conversely, for the longitudinal (series) current $\mathbf{I}_T$ we can relate it to the voltage drop along the electrode which in turn can be related to the node voltages with respect to a point far from the electrode as

$$\mathbf{Z}_L \cdot \mathbf{I}_L = \mathbf{m}_B \cdot \mathbf{V}_n \tag{13}$$

where $\mathbf{m}_B$ have elements with the following structure

- $\mathbf{m}_B(i,k) = 1$ if node j is connected to the beginning of segment k;
- $\mathbf{m}_B(i,k) = -1$ if node j is connected to the ending of segment k;
- $\mathbf{m}_B(i,k) = 0$ if node j is not connected to segment k.

Assuming a vector of external currents injected in the electrodes $\mathbf{I}_e$, and applying Kirchoff's law to the electrodes leads to

$$\mathbf{I}_e = \mathbf{m}_B^T \cdot \mathbf{I}_L + \mathbf{m}_A^T \cdot \mathbf{I}_T \quad . \tag{14}$$

Then using (12) and (13) it is possible to write

$$\mathbf{I}_e = \left(\mathbf{m}_A^T \cdot \mathbf{Z}_T^{-1} \cdot \mathbf{m}_A + \mathbf{m}_B^T \cdot \mathbf{Z}_L^{-1} \cdot \mathbf{m}_B\right) \cdot \mathbf{V}_n = \mathbf{Y}_{eq} \cdot \mathbf{V}_n \tag{15}$$

where $\mathbf{Y}_{eq}$ is the equivalent nodal admittance matrix for a system of electrodes.

D. Rational Approximation

The rational approximation of $\mathbf{Y}_{eq}$ is carried out using the so-called Vector Fitting (VF) algorithm, thus it is approximated by

$$\mathbf{Y}_{eq}(s) \approx \sum_{n=1}^{N} \frac{\mathbf{R}_n}{s + p_n} + \mathbf{D} + s\mathbf{E} \tag{16}$$

where $\mathbf{D}$ and $\mathbf{E}$ are real matrices, the poles p_n are either real or come in complex conjugates and the same can be said about the elements in $\mathbf{R}_n$. To ensure that the rational approximation is a feasible realization, one has to ensure that it is passive. This can be achieved by a post-processing set of routines to enforce passivity. In the literature there have been several approaches to achieve that. Here, the fast passivity enforcement by perturbation of the residue matrix eigenvalues was considered [20].

To improve the passivity enforcement it was found that it is better to pre-calculated $\mathbf{D}$ and $\mathbf{E}$ as

$$\mathbf{D} + s_\infty \mathbf{E} = \Re\left(\mathbf{Y}_{eq}(\infty)\right) + s_\infty \Im\left(\mathbf{Y}_{eq}(\infty)\right) \tag{17}$$

where, from a practical point of view, it was considered a very high frequency, i.e., $s_\infty = j2\pi\,10^{10}$ for the evaluation of $\mathbf{Y}_{eq}(\infty)$. Then the rational approximation is calculated as a strictly proper function. It is important to note that for aerial conductors $\Im(\mathbf{Y}_{eq}(\infty)) \approx$ null and the procedure becomes rather similar to what was used in [21] to represent nonuniform overhead lines.

III. Test Cases

In the test cases presented in this section, we calculate $\mathbf{Y}_{eq}$ in a predefined frequency range using HEM and compared this results to the one obtained via rational approximation. For the time responses, the Numerical Laplace Transform (NLT) [22]–[26] was applied with HEM and the recursive convolution [12,13,27] with the proposed algorithm.

A. Short horizontal conductor over copper plate

This test is based on the configuration used in [28]. The layout of the used experimental setup is depicted in Fig. 3. Here, it is assumed that the copper plate allows to consider an ideal image plane. The lead wire has an approximate length of 50 cm and the horizontal wire has a 50 cm constant height. The pulse generator (PG) was represented as a piecewise linear voltage source as in [28].

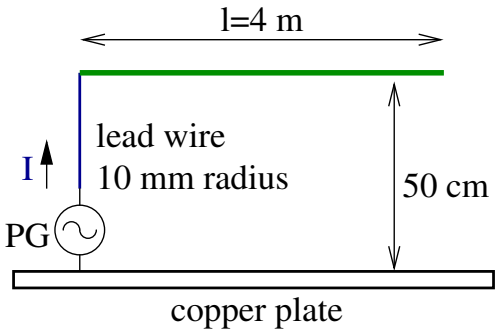

Fig. 3. Finite length conductor over an copper plate.

The first step is then obtaining the equivalent nodal admittance matrix, $\mathbf{Y}_{eq}(s)$. A key issue is the conductor segmentation. If very short segments are considered, a very large $\mathbf{Y}_{eq}(s)$ is needed. This is a challenge to accurate and passive rational fitting. Here it was considered that the segment length should be close to 10 times the conductor radius. This led to a total of 30 segments, being 5 for the lead wire and 25 for the horizontal conductor, thus $\mathbf{Y}_{eq}(s)$ is a 31×31 matrix. A frequency sweep from 1 MHz to 1 GHz with 250 samples was used for the fitting.

Given the rather small electrodes involved due to segmentation, adjacent electrodes present very similar admittances, e.g., $Y_{eq}(s)_{12} \approx Y_{eq}(s)_{12}$. Thus to avoid a

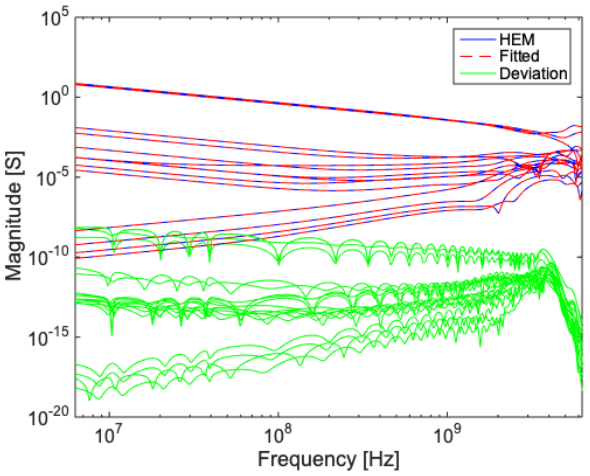

Fig. 4. Comparison of fitted admittances.

"blurry" picture Figure 4 depicts only some elements in $\mathbf{Y}_{eq}(s)$, calculated using HEM, th proposed model (labeled as "fitted") and the deviation found. Although this figure shows only every 5th element on each row and column, the fitting was rather accurate for the complete $\mathbf{Y}_{eq}(s)$ as the RMS-error was 6.4E-10. Only one passivity violation was found which was easily removed by residue perturbation as implemented in the *RPDriver* of the Matrix Fitting toolbox available at https://www.sintef.no/projectweb/vectfit/. A challenge in this procedure is a very time consuming routine due to the large dimension of the matrices involved. Alternatively, one could consider using the approach recently proposed in [29] as it reports lower computation burden to assess passivity violations and to modify the rational approximation.

As the number of segments used in each conductor involved is a key element in the order of the equivalent nodal admittance matrix, a metric should be developed to adequate the segmentation to the type of phenomena being considered. Alternatively, an adaptative segmentation scheme, a coarse segmentation for conductors away from the region of interest and a fine segmentation to the region of interest.

The time-domain responses to the voltage pulse were computed. Figure 5 presents the voltage at the connection between the horizontal and vertical conductors while the injected current is presented in Fig. 6. It can be observed a very good agreement for the voltage waveform, while for the current there are some small deviations. These could be reduced if, instead an ideal ground plane, the actual copper plate is represented.

B. Nonuniform Overhead Circuit

A nonuniform overhead line occurs whenever one cannot neglect the variation of the per unit length parameters along the circuit. Typically, this can be approximated by a cascade of uniform lines, each calculated assuming a constant height. However, if the segment length is in order of magnitude of the conductors height, the quasi-TEM hypothesis are not met.

Similarly to the previous case, the first step lies in obtaining the equivalent nodal admittance matrix considering

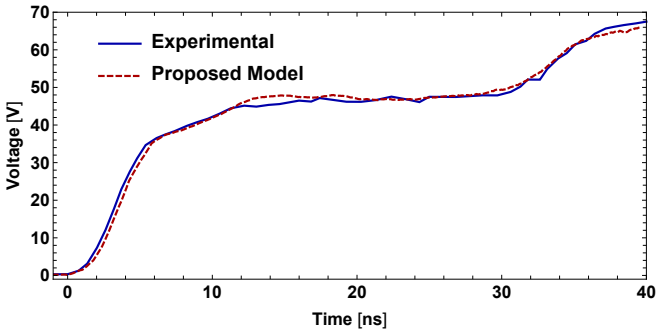

Fig. 5. Comparison of simulated and measured voltages.

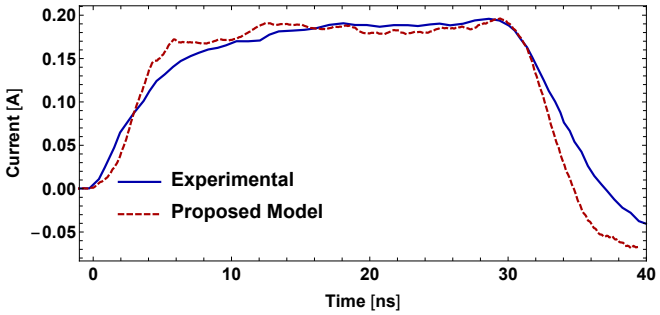

Fig. 6. Comparison of simulated and measured currents.

the conductors catenary. The expression for the catenary is

$$y = q\left(\cosh\frac{x}{\ell} - 1\right) \tag{18}$$

where y is the actual height of the conductors, ℓ is the length of the line span and q is a parameter related to the specific weight of the conductor, (q=1.73 for the phase conductors while it is 4.26 km for the ground-wires). Here, it is considered the actual crossing of the Amazon river as depicted in Fig. 7.

(a) actual tower

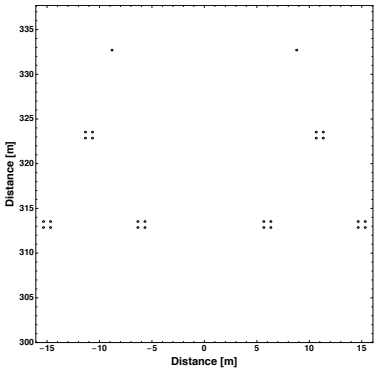

(b) conductors arrangment

Fig. 7. Nouniform overhead transmission line.

The line voltage is 500 kV. Each phase has a four conductor bundle with 0.457 mm spacing. The span ℓ between adjcent towers in the river crossing is around 2.1 km, the sag is around 300 m. The heights of bundle centers are 313.2 m and 323.2 m. The ground wires height are 332.7 m. Phase conductors have a 29.591 mm diameter, and ground wires are 3/8" EHS. The horizontal distance between phase conductors is 5 m, and

between ground wires is 17.6 m. The river was assumed with a constant resistivity, i.e., without frequency dependency of roughly 20 Ωm.

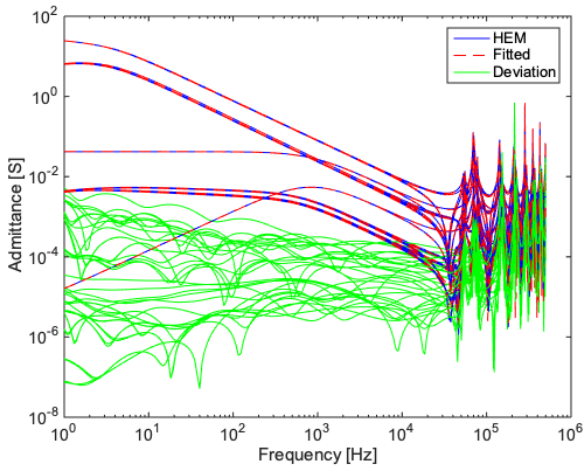

Fig. 8. Fitting the equivalent nodal admittance matrix for a wide river crossing of an overhead transmission line.

The time responses to a double exponential applied voltage to the outermost phase conductor is presented in Fig. 9. It can be observed a very good agreement between the results obtained with HEM and the proposed approach.

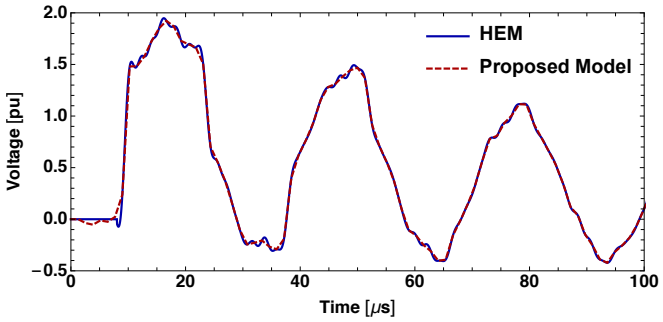

Fig. 9. Time responses obtained using rational approximation and using HEM.

IV. Conclusions

This work proposes a procedure based on rational approximation for the inclusion of elements based on electromagnetic field formulation, thus allowing a concrete realization of wideband modeling of aerial conductors in arbitrary orientation.

There are three main steps in the proposed procedure: the derivation of the equivalent nodal admittance matrix which must be carried out independently in the frequency domain, the derivation of the rational approximation and its passive enforcement. There are some challenges in the realization of a large admittance matrix that might occur in some configurations.

For the test cases considered here, the frequency domain functions were rather smooth in all the range of interest. The time responses indicate that the rational approximation attained an excellent accuracy when compared with the results obtained using the NLT. In the comparison with experimental results, some minor discrepancies were found, probably related to assuming the copper plate as an ideal plane.